

# Activation of Cannabinoid Type 2 Receptors Inhibits HIV-1 Envelope Glycoprotein gp120-Induced Synapse Loss

Hee Jung Kim, Angela H. Shin, and Stanley A. Thayer

Department of Pharmacology, University of Minnesota Medical School, Minneapolis, Minnesota (H.J.K., A.H.S., S.A.T.); and Department of Physiology, College of Medicine, Dankook University, Cheonan, Chungnam, Korea (H.J.K.)

Received February 8, 2011; accepted June 13, 2011

## ABSTRACT

HIV-1 infection of the central nervous system is associated with dendritic and synaptic damage that correlates with cognitive decline in patients with HIV-1-associated dementia (HAD). HAD is due in part to the release of viral proteins from infected cells. Because cannabinoids modulate neurotoxic and inflammatory processes, we investigated their effects on changes in synaptic connections induced by the HIV-1 envelope glycoprotein gp120. Morphology and synapses between cultured hippocampal neurons were visualized by confocal imaging of neurons expressing DsRed2 and postsynaptic density protein 95 fused to green fluorescent protein (PSD95-GFP). Twenty-four-hour treatment with gp120 IIIB decreased the number of PSD95-GFP puncta by  $37 \pm 4\%$ . The decrease was concentration-dependent ( $EC_{50} = 153 \pm 50$  pM). Synapse loss preceded cell death as defined by retention of DsRed2 fluorescence gp120 activated CXCR4 on microglia to evoke interleukin-1 $\beta$  (IL-1 $\beta$ ) release. Pharmacological studies de-

termined that sequential activation of CXCR4, the IL-1 $\beta$  receptor, and the *N*-methyl-D-aspartate receptor was required. Expression of alternative reading frame polypeptide, which inhibits the ubiquitin ligase murine double minute 2, protected synapses, implicating the ubiquitin-proteasome pathway. Cannabimimetic drugs are of particular relevance to HAD because of their clinical and illicit use in patients with AIDS. The cannabinoid receptor full agonist [(*R*)-(+)-[2,3-dihydro-5-methyl-3[(4-morpholinyl)methyl]pyrrolo[1,2,3-*de*]-1,4-benzoxazinyl]-(1-naphthalenyl) methanone mesylate salt] (Win55,212-2) inhibited gp120-induced IL-1 $\beta$  production and synapse in a manner reversed by a cannabinoid type 2 receptor antagonist. In contrast, Win55,212-2 did not inhibit synapse loss elicited by exposure to the HIV-1 protein Tat. These results indicate that cannabinoids prevent the impairment of network function produced by gp120 and, thus, might have therapeutic potential in HAD.

## Introduction

Over 30 million people are infected with HIV-1, the cause of AIDS. HIV-associated dementia (HAD) is one of the most important complications associated with AIDS because this neuropsychiatric disorder eventually impairs the patient's

This work was supported by the National Institutes of Health National Institute on Drug Abuse [Grants DA07304, DA11806, DA07234]; and the National Science Foundation [Grant IOS0814549].

A preliminary version of this report was presented in abstract form (Kim H and Thayer SA. Cannabinoids inhibit gp120-induced synapse loss. *Soc Neurosci Abstr* 35:727.19, 2009).

Article, publication date, and citation information can be found at <http://molpharm.aspetjournals.org>.  
doi:10.1124/mol.111.071647.

ability to perform even the most simple functions of daily living (Heaton et al., 2011). The successful development of combination antiretroviral therapy has increased the survival and improved the quality of life for patients with AIDS. However, despite initial improvement of patients with HAD receiving combination antiretroviral therapy, the prevalence of HIV-associated neurocognitive disorders (HAND) is increasing, in part because of the prolonged lifespan of infected patients (Heaton et al., 2011).

HIV-1 can productively infect macrophages and microglia but not neurons. Thus, the neurotoxicity produced by HIV-1 in the central nervous system is indirect, resulting from shed viral proteins, released excitotoxins and secreted inflamma-

**ABBREVIATIONS:** HAD, HIV-associated dementia; HAND, HIV-associated neurocognitive disorders; CB1, cannabinoid type 1 receptor; CB2, cannabinoid type 2 receptor; PSD, postsynaptic density protein; PSD95-GFP, postsynaptic density protein 95 fused to green fluorescent protein; ARF, alternative reading frame polypeptide; DMEM, Dulbecco's modified Eagle's medium; MK801, dizocilpine; Win55212-2, [(*R*)-(+)-[2,3-dihydro-5-methyl-3[(4-morpholinyl)methyl]pyrrolo[1,2,3-*de*]-1,4-benzoxazinyl]-(1-naphthalenyl) methanone mesylate salt]; AM630, 6-iodo-2-methyl-1-[2-(4-morpholinyl)ethyl]-1*H*-indol-3-yl(4-methoxyphenyl)methanone; AMD3100, 1,1'-[1,4-phenylenebis(methylene)]bis-1,4,8,11-tetraazacyclotetradecane octahydrochloride; TKP, threonine-lysine-proline; HHSS, HEPES-buffered Hanks' salt solution; qRT-PCR, quantitative real-time polymerase chain reaction; nNOS, neuronal nitric-oxide synthase; PCR, polymerase chain reaction; IL-1 $\beta$ , interleukin-1 $\beta$ ; L-NAME, *N*<sup>G</sup>-nitro-L-arginine methyl ester hydrochloride; nutlin-3, ( $\pm$ )-4-[4,5-bis(4-chlorophenyl)-2-(2-isopropoxy-4-methoxy-phenyl)-4,5-dihydro-imidazole-1-carbonyl]-piperazin-2-one; ELISA, enzyme-linked immunosorbent assay; NMDA, *N*-methyl-D-aspartate; PBS, phosphate-buffered saline; BSA, bovine serum albumin; GFP, green fluorescent protein; ANOVA, analysis of variance; PI, propidium iodide; gp120, glycoprotein 120.

tory cytokines that act on neurons (Kaul et al., 2005). The HIV-1 envelope protein gp120 is of particular interest because it is shed by infected cells (Schneider et al., 1986) and is a potent neurotoxin (Dawson et al., 1993). The neurotoxic effects of gp120 are mediated through an NMDA receptor-dependent mechanism (Dawson et al., 1993) via both direct actions on neurons (Pattarini et al., 1998) and indirect mechanisms (Kaul and Lipton, 1999).

Cognitive impairment in patients with HAD correlates better with dendritic changes than neuronal death (Sá et al., 2004). gp120 produces dendritic pruning and loss of spines when applied to neurons in culture or expressed in transgenic animals (Toggas et al., 1994; Viviani et al., 2006). We have found previously that glutamate and the HIV protein Tat induce synapse loss via a mechanism that is distinct from that leading to cell death (Kim et al., 2008a; Waataja et al., 2008). Indeed, we speculate that loss of excitatory synapses during exposure to certain neurotoxic stimuli may be a form of homeostatic scaling that actually affords protection from excessive stimulation. Whether gp120 evokes synapse loss via this mechanism is not known.

Cannabimimetic drugs are of particular relevance to AIDS because these drugs are used clinically to prevent nausea and wasting in these patients (Plasse et al., 1991), and anecdotal reports suggest high marijuana usage by individuals with AIDS (James, 1999). Cannabinoid drugs exhibit neuroprotective properties in some models (Shen and Thayer, 1998; Kim et al., 2008b) and the endocannabinoid system is believed to provide on-demand neuroprotection (Marsicano et al., 2003). We have found previously that cannabinoid receptor agonists prevent and can even reverse synapse loss induced by epileptiform activity (Kim et al., 2008b).

Here, we examined the effects of HIV-1 gp120 on synaptic connections between hippocampal neurons in culture. The mechanism of synapse loss was indirect, requiring cytokine release from non-neuronal cells. This loss was mediated via NMDA receptors, but the downstream mechanism was distinct from that leading to cell death. Finally, we examined the effects of cannabinoids on this process and found that activation of cannabinoid type 2 (CB2) receptors prevented gp120-induced synapse loss, consistent with inhibition of the release of an inflammatory cytokine.

## Materials and Methods

**Materials.** Materials were obtained from the following sources: the PSD95-GFP expression vector (pGW1-CMV-PSD95-EGFP) was kindly provided by Donald B. Arnold; the alternative reading frame polypeptide (ARF) expression vector (pcDNA3-myc-ARF) was kindly provided by Yanping Zhang; the expression vector for DsRed2 (pDsRed2-N1) was from Clontech (Mountain View, CA); HIV-1 gp120 IIIB was from Protein Sciences Corporation (Meriden, CT); Dulbecco's modified Eagle's medium (DMEM), fetal bovine serum, and horse serum were from Invitrogen (Carlsbad, CA); IL-1- $\alpha$  was from R&D Systems (Minneapolis, MN); dizocilpine (MK-801), [(R)-(+)-[2,3-dihydro-5-methyl-3[(4-morpholinyl)methyl]pyrrolo[1,2,3-de]-1,4-benzoxazinyl]-(1-naphthalenyl) methanone mesylate salt] (Win55,212-2), 6-iodo-2-methyl-1-[2-(4-morpholinyl)ethyl]-1*H*-indol-3-yl(4-methoxyphenyl)methanone (AM630), 1,1'-[1,4-phenylenebis(methylene)]bis-1,4,8,11-tetraazacyclotetradecane octahydrochloride (AMD3100), threonine-lysine-proline (TKP), and all other reagents were from Sigma-Aldrich (St. Louis, MO). PSD95-GFP lacking the PEST sequence (PSD95 $\Delta$ PEST-GFP) was produced by QuikChange Site-Directed mutagenesis (Stratagene, La Jolla, CA); primers were designed to delete

amino acids 10 to 25 of rat PSD-95 as described previously (Kim et al., 2008a).

**Cell Culture.** Rat hippocampal neurons were grown in primary culture as described previously (Kim et al., 2008a) with minor modifications. Fetuses were removed on embryonic day 17 from maternal rats, anesthetized with CO<sub>2</sub>, and sacrificed by decapitation. Hippocampi were dissected and placed in Ca<sup>2+</sup> and Mg<sup>2+</sup>-free HEPES-buffered Hanks' salt solution, pH 7.45. HEPES-buffered Hanks' salt solution was composed of the following: 20 mM HEPES, 137 mM NaCl, 1.3 mM CaCl<sub>2</sub>, 0.4 mM MgSO<sub>4</sub>, 0.5 mM MgCl<sub>2</sub>, 5.0 mM KCl, 0.4 mM KH<sub>2</sub>PO<sub>4</sub>, 0.6 mM Na<sub>2</sub>HPO<sub>4</sub>, 3.0 mM NaHCO<sub>3</sub>, and 5.6 mM glucose. Cells were dissociated by trituration through a 5-ml pipette and a flame-narrowed Pasteur pipette, pelleted, and resuspended in DMEM without glutamine, supplemented with 10% fetal bovine serum and penicillin/streptomycin (100 U/ml and 100  $\mu$ g/ml, respectively). Dissociated cells were then plated at a density of 100,000 to 200,000 cells/dish onto a 25-mm round coverglass (#1) glued to cover a 19-mm diameter opening drilled through the bottom of a 35-mm Petri dish. The coverglass was precoated with Matrigel (200  $\mu$ l, 0.2 mg/ml). Neurons were grown in a humidified atmosphere of 10% CO<sub>2</sub> and 90% air, pH 7.4, at 37°C, and fed on days 1 and 6 by exchange of 75% of the media with DMEM, supplemented with 10% horse serum and penicillin/streptomycin. Cells used in these experiments were cultured without mitotic inhibitors for at least 12 days.

**Immunocytochemistry.** Neuronal cultures were prepared as described above and fixed between day 13 and 14 in vitro. Cells were stained with 1  $\mu$ M Hoechst 33342 (Sigma-Aldrich) for 15 min at 37°C, washed with PBS, and fixed with ice-cold methanol for 10 min at -20°C. Cells were washed with PBS three times and blocked for 1 h at room temperature in 10% bovine serum albumin (BSA; Sigma-Aldrich) in PBS. After blocking, cells were incubated with affinity-purified antibodies in PBS containing 3% BSA for 16 h at 4°C. The following antibodies were used: mouse anti-MAP2 (Sigma-Aldrich, 1:400 titer), mouse anti-glial fibrillary acidic protein (Sigma-Aldrich, 1:400 titer), or mouse anti-OX42 (AbCam, Cambridge, UK; 1:200 titer) to identify neurons, astrocytes, or microglia, respectively. Immunolabeled cells were visualized by incubating with fluorescein isothiocyanate-conjugated anti-mouse antibody (Dako Denmark A/S, Glostrup, Denmark; 1:300 titer) in PBS containing 3% BSA for 1 h at room temperature. Coverslips were mounted in Fluoromount (Southern Biotech, Birmingham, AL). Images of immunolabeled cells were captured on an Olympus IX70 inverted microscope (Olympus America, Melville, NY) equipped with a 20 $\times$  objective (0.4 numerical aperture), a charge-coupled device camera (DVC Co., Austin, TX), and DVC View software (version 2.2.8). Fluorescein isothiocyanate was excited at 455 to 495 nm, and emission was collected at 510 nm. Hoechst 33342 was excited at 330 to 385 nm and emission was collected at 420 nm. In each region, the total number of Hoechst-stained cells was counted (100%) and compared with the number of cells labeled with primary antibody to calculate the percentage of each cell type. At least six separate images were counted for each cell type over two different cultures.

**Transfection.** Rat hippocampal neurons were transfected between 10 and 13 days in vitro using a modification of a protocol described previously (Kim et al., 2008a). In brief, hippocampal cultures were incubated for at least 20 min in DMEM supplemented with 1 mM kynurenic acid, 10 mM MgCl<sub>2</sub>, and 5 mM HEPES to reduce neurotoxicity. A DNA/calcium phosphate precipitate containing 1  $\mu$ g of plasmid DNA per well was prepared, allowed to form for 30 min at room temperature, and added to the culture. After a 90-min incubation, cells were washed once with DMEM supplemented with MgCl<sub>2</sub> and HEPES and then returned to conditioned media, saved at the beginning of the procedure. The transfection efficiency ranged from 2 to 11% based on the percentage of neurons that expressed DsRed2.

**Confocal Imaging.** Transfected neurons were transferred to the stage of a laser-scanning confocal microscope (Olympus Fluoview 300) and viewed through a 60 $\times$  oil-immersion objective (numerical

aperture, 1.40). Because of the low transfection efficiency, only one cell in the field expressed fluorescent proteins. For experiments in which the same neuron was imaged before and after a 24-h interval, the location of the cell was recorded using micrometers attached to the stage of the microscope. Nine optical sections spanning 8  $\mu\text{m}$  in the  $z$ -dimension were collected (1- $\mu\text{m}$  steps) and combined through the  $z$ -axis into a compressed  $z$  stack. GFP was excited at 488 nm with an argon ion laser, and emission was collected at 530 nm (10 nm bandpass). The excitation (HeNe laser) and emission wavelengths for DsRed2 were 543 nm and  $>605$  nm, respectively.

**Image Processing.** To count and label PSD95-GFP puncta, an automated algorithm was created using MetaMorph 6.2 image processing software (Molecular Devices, Sunnyvale, CA) described previously (Waataja et al., 2008). In brief, maximum  $z$ -projection images were created from the DsRed2 and GFP image stacks. Next, a threshold set 1 S.D. above the image mean was applied to the DsRed2 image. This created a one-bit image that was used as a mask via a logical AND function with the GFP maximum  $z$ -projection. A top-hat filter (80 pixels) was applied to the masked PSD95-GFP image. A threshold set 1.5 S.D. above the mean intensity inside the mask was then applied to the contrast-enhanced image. Structures between 8 and 80 pixels (approximately 0.37–3.12  $\mu\text{m}$  in diameter) were counted as PSDs. The structures were then dilated and superimposed on the DsRed2 maximum  $z$ -projection for visualization. PSD counts were presented as mean  $\pm$  S.E.M., where  $n$  is the number of cells, each from a separate coverglass over multiple cultures. We used Student's  $t$  test for single or ANOVA with Bonferroni post test for multiple statistical comparisons.

**Toxicity.** Cell death was quantified using propidium iodide (PI) fluorescence as described previously (Kim et al., 2008a). Cell culture was performed as described above except that 100,000 cells/well were plated in 96-well plates and grown for 12 to 14 days in vitro. The experiment was started by replacing 100  $\mu\text{l}$  (approximately two-thirds volume) of the cell culture medium with fresh DMEM containing 10% horse serum, penicillin/streptomycin, 70  $\mu\text{M}$  PI, and either neurotoxin (1 mM glutamate or gp120 at various concentrations) or vehicle (control). The plate was placed in a FluoStar Galaxy multiwell fluorescent plate scanner (BMG Technologies GmbH, Offenbourg, Germany) and maintained at 37°C. PI fluorescence intensity measurements (excitation 544 nm  $\pm$  15, emission 620 nm  $\pm$  15) were taken at times 0, 24, and 48 h. Between measurements, cells were returned to the incubator and kept at 37°C in 10% CO<sub>2</sub>. Drugs, when present, were applied 15 min before application of the neurotoxin and included in the media exchange. Each treatment was performed in triplicate; thus, a set of three wells from a single plating of cells was defined as an individual experiment ( $n = 1$ ).

**ELISA.** IL-1 $\beta$  protein levels were determined using a commercially available rat IL-1 ELISA kit (R&D Systems). The assays were performed according to the manufacturer's instructions. Absorbance was read at 450 nm using a FluoStar Galaxy multiwell fluorescent plate scanner (BMG Technologies GmbH). The concentration of secreted IL-1 $\beta$  is expressed as picograms per milliliter.

**Quantitative Real-Time Reverse Transcription-PCR.** RNA was extracted from cultures using an RNA isolation kit (Zymo Research, Irvine, CA). For real-time PCR, RNA was amplified using a SYBR Green Brilliant II qRT-PCR kit (Stratagene) following the manufacturer's recommendations. In brief, 12.5  $\mu\text{l}$  of SYBR Green qRT-PCR master mix was combined with 100 ng of isolated RNA, 100 nM sense and antisense primers, and 1  $\mu\text{l}$  of RT/RNase block enzyme mix. Reverse transcription was performed by incubating samples at 50°C for 30 min. Samples were then transferred into an MX3005P cycler. Samples were monitored using MxPro-Mx3005P version 4.01 (Stratagene) software during the following thermocycling protocol: initial denaturation, 95°C for 10 min, followed by 40 cycles of 95°C for 30 s, and 60°C for 1 min. IL-1 $\beta$  was amplified using primers 5'-GGAAGGCAGTGTCACTCATTTGTGG-3' and 5'-CAGCTCACATGGGTCAGACAGCAC-3' that were designed as shown previously (Nam et al., 2008). As an internal reference control, the

glyceraldehyde-3-phosphate dehydrogenase gene was PCR-amplified using QuantiTect primers (QIAGEN, Valencia, CA). For each sample, two IL-1 $\beta$  reactions and two glyceraldehyde-3-phosphate dehydrogenase reactions were run in parallel and averaged ( $n = 1$ ). Quantitative analysis was performed using the  $2^{-\Delta\Delta C_t}$  method.

## Results

**gp120 Induces Synapse Loss.** We have described previously a quantitative assay to track changes in the number of postsynaptic sites visualized by confocal imaging of hippocampal neurons expressing PSD95-GFP and DsRed2 (Waataja et al., 2008). Figure 1A shows representative images of neurons 48 h after transfection with expression plasmids for PSD95-GFP and DsRed2. PSD95-GFP expressed as discrete puncta that contrasted well from diffuse green fluorescence found throughout the cell. DsRed2 expression filled the soma and dendrites and was used to track morphological changes, as a mask for image processing and to determine cell viability based on cytoplasmic retention of the fluorescent protein. Image processing identified and counted puncta by locating intensity peaks of the appropriate size (mean diameter = 0.52  $\mu\text{m}$ ) in contact with the DsRed2 mask. In a series of previously published control experiments, we demonstrated that PSD95-GFP puncta represent functional postsynaptic sites as indicated by colocalization with neurotransmitter release sites, NMDA-induced Ca<sup>2+</sup> increases, and NMDA receptor immunoreactivity (Waataja et al., 2008).

We investigated the effects of gp120 on the number of synaptic connections between hippocampal neurons in culture. Treatment with 600 pM gp120 for 24 h induced a  $37 \pm 4\%$  ( $n = 44$ ) loss of PSD95-GFP puncta (Fig. 1A). The time course of gp120-induced changes in the number of fluorescent puncta is shown in Fig. 1B. A 24-h exposure to gp120 significantly decreased the number of synaptic sites. gp120-induced synapse loss was concentration-dependent with an EC<sub>50</sub> of  $153 \pm 50$  pM (Fig. 1C). Treatment with gp120 for 24 h did not significantly affect cell survival relative to control as defined by retention of dsRed (Fig. 1A) and uptake of propidium iodide (Fig. 1D). However, by 48 h, gp120 elicited significant cell death (EC<sub>50</sub> =  $85 \pm 45$  pM). These findings suggest that synapse loss preceded neuronal death.

**gp120-Induced Synapse Loss Requires Sequential Activation of CXCR4, the IL-1 Receptor, and the NMDA Receptor.** gp120 exerts neurotoxic effects by both direct actions on neurons (Pattarini et al., 1998) and indirect actions via the evoked release of cytokines from glia (Kaul and Lipton, 1999). Immunocytochemistry experiments revealed that the hippocampal cultures used for these studies were composed of  $18 \pm 2\%$  neurons,  $70 \pm 3\%$  astrocytes, and  $9 \pm 3\%$  microglia. To determine whether gp120 was acting indirectly on microglia present in the mixed cultures studied here, we pretreated the cultures with the tuftsin-derived tripeptide TKP that inhibits microglial activation (Auriault et al., 1983) (Fig. 2A). TKP (50  $\mu\text{M}$ ) blocked gp120-induced synapse loss, implicating microglia as the primary target for gp120. The initial number of PSDs was  $67 \pm 8$  and increased to  $75 \pm 16$  after treatment with TKP. The IIIB strain of gp120 used in the present study binds to the chemokine receptor CXCR4 (Hesselgesser et al., 1998). Thus, we tested the CXCR4 receptor antagonist AMD3100, which prevents HIV-1 entry, to investigate the role of CXCR4 in gp120-



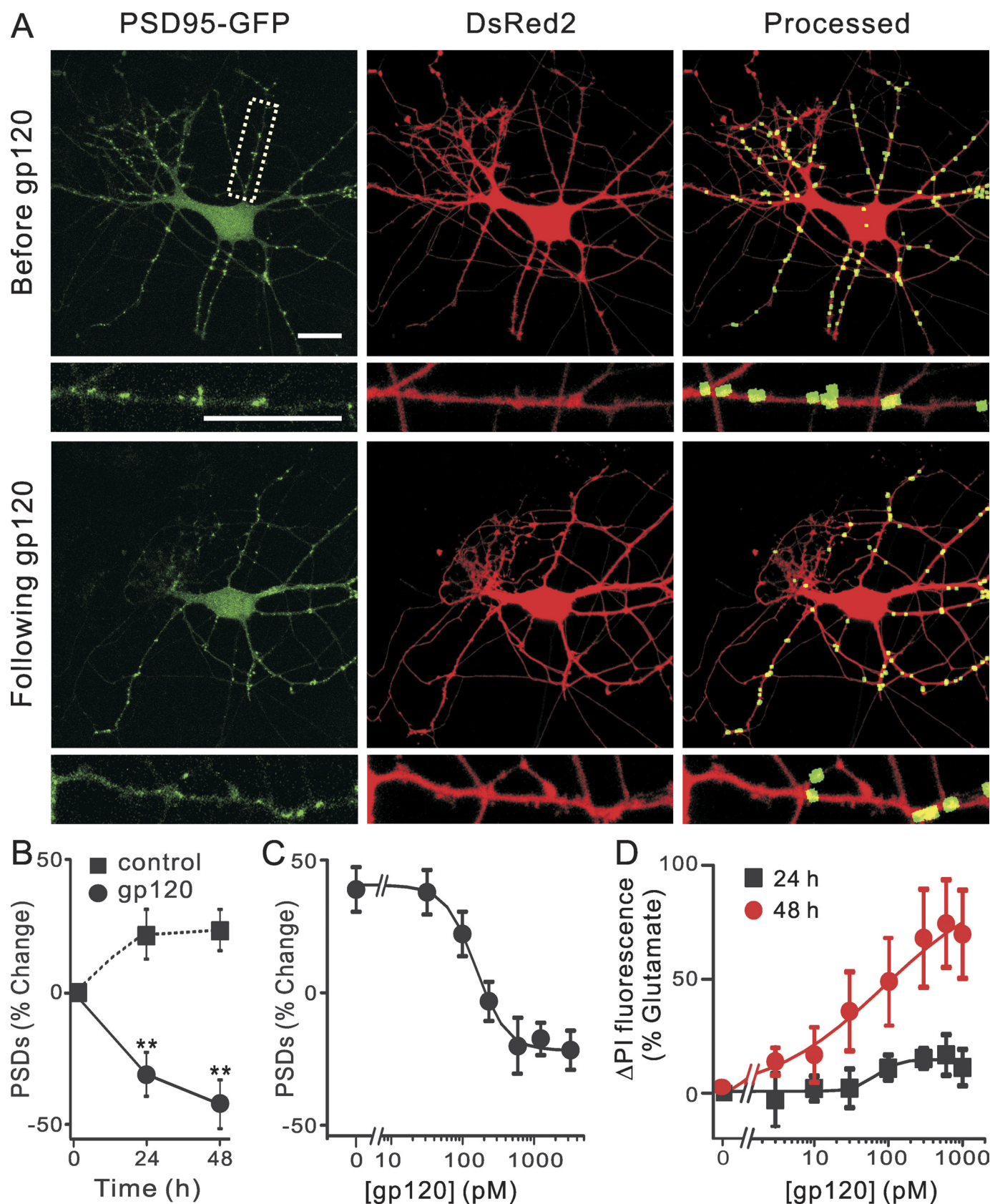


**Fig. 1.** HIV-1 gp120 IIIB induced PSD loss and cell death in a time and concentration-dependent manner. **A**, confocal fluorescent images display maximum *z*-projections of neurons expressing PSD95-GFP and DsRed2 before and 24 h after treatment with 600 pM gp120. Processing of PSD95-GFP images identified PSDs as fluorescent puncta meeting intensity and size criteria and in contact with a mask derived from the DsRed2 image. Labeled PSDs were dilated and overlaid on the DsRed2 image for visualization purposes (processed). Insets, enlarged images of the boxed region. Scale bars, 10  $\mu$ m. **B**, graph shows time-dependent changes in the number of PSD95-GFP puncta for untreated cells (control, ■) and cells treated with 600 pM

induced synapse loss (Donzella et al., 1998). Pretreatment with AMD3100 (1  $\mu$ M) significantly reduced gp120-induced synapse loss, indicating that CXCR4 was required. Both direct and indirect neurotoxicity elicited by gp120 requires the activation of NMDA receptors (Dawson et al., 1993; Pattarini et al., 1998; Kaul and Lipton, 1999). Similar to the mecha-

nism of gp120-induced cell death, pretreatment with dizocilpine (MK801; 10  $\mu$ M) blocked gp120-induced synapse loss. If gp120 acts indirectly, as suggested by the TKP experiment, then microglia-derived cytokines might act on neurons to activate NMDA receptors. Indeed, application of the endogenously produced IL-1 receptor antagonist, IL-1-ra, completely prevented gp120-induced synapse loss (Fig. 2A), suggesting the activation of IL-1 receptors expressed by neurons (Viviani et al., 2006).

If the synapse loss induced by gp120 is mediated by IL-1 $\beta$  receptors, then IL-1 $\beta$  should mimic the effects of gp120. Exogenous application of IL-1 $\beta$  (3 ng/ml) induced a loss of PSD95-GFP puncta, which was abolished by 1  $\mu$ g/ml IL-1-ra (Fig. 2B). In contrast to the actions of gp120, IL-1 $\beta$ -induced synapse loss was not affected by pretreatment with 1  $\mu$ M AMD3100, consistent with the idea that CXCR4 is upstream from the IL-1 $\beta$  receptor. Activation of IL-1 $\beta$  receptors stimulates the tyrosine kinase Src (Viviani et al., 2003), which phosphorylates NMDA receptors and sensitizes them to glutamate (Viviani et al., 2006; Salter et al., 2009). Here, we show that pretreatment with 10  $\mu$ M MK801 or 10  $\mu$ M pyrazolopyrimidine 2, a specific inhibitor of Src family kinases, prevented IL-1 $\beta$ -induced synapse loss (Fig. 2B). These results suggest that gp120-induced release of IL-1 $\beta$  from microglia might lead to the loss of synaptic connections as a result of overstimulation of NMDA receptors.

This hypothesis predicts that gp120 will elevate IL-1 $\beta$  levels in hippocampal cultures. Treating hippocampal cultures with 600 pM gp120 led to a 25-fold increase in IL-1 $\beta$  as detected by ELISA (Fig. 3A). This result is consistent with previous studies showing that infection with HIV-1 IIIB or intracerebroventricular microinfusion of gp120 induced glial release of IL-1 $\beta$  (Merrill et al., 1992; Ilyin and Plata-Salamán, 1997). IL-1 $\beta$  measured in the media collected from gp120-treated hippocampal cultures was near the limit of detection with commercially available ELISAs (Fig. 3A). Because the evoked release of IL-1 $\beta$  is accompanied by increased transcription of IL-1 $\beta$  message, we used a qRT-PCR assay to measure IL-1 $\beta$  production. Treating hippocampal cultures with 600 pM gp120 evoked a time-dependent increase in the expression of IL-1 $\beta$  mRNA that peaked 12 h after gp120 treatment (Fig. 3B). Thus, subsequent assays were performed at 12 h. Increases in IL-1 $\beta$  mRNA were blocked by pretreatment with either TKP or AMD3100 (Fig. 3C), suggesting that gp120 acts via CXCR4 on microglia to evoke IL-1 $\beta$  production and subsequent synapse loss.

**The gp120-Induced Loss of PSD95-GFP Puncta Is Mediated by the Ubiquitin-Proteasome Pathway.** In a previous study, gp120 was shown to reduce spine density and corresponding PSD95 levels (Viviani et al., 2006). We have found that activation of NMDA receptors results in the loss of postsynaptic sites by activation of the ubiquitin-proteasome

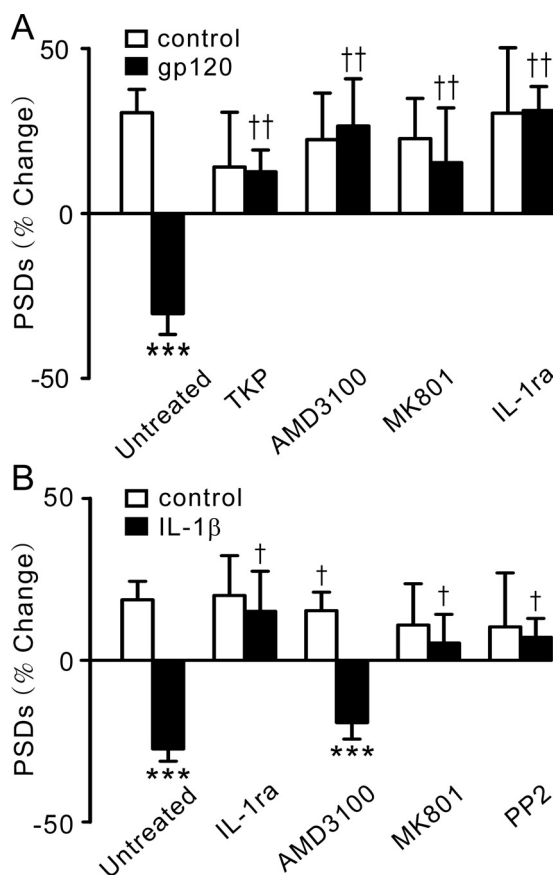


**Fig. 2.** gp120-induced synapse loss required sequential activation of CXCR4, IL-1 $\beta$ , and NMDA receptors. A, inhibition of CXCR4, IL-1 $\beta$ , or NMDA receptors prevents gp120-induced synapse loss. Bar graph summarizes changes in PSD95-GFP puncta (PSDs) after 24-h treatment under control (□) or gp120-treated (■) conditions in the absence (untreated,  $n = 24$ ) or presence of the indicated inhibitors. Cultures were treated with either 50  $\mu$ M TKP ( $n = 13$ ), 1  $\mu$ M AMD3100 ( $n = 6$ ), or 10  $\mu$ M MK801 ( $n = 7$ ) for 30 min before the addition of gp120 or cotreated with 1  $\mu$ g/ml IL-1-ra ( $n = 6$ ) and gp120. Data are expressed as mean  $\pm$  S.E.M. \*\*\*,  $p < 0.001$  relative to control, Student's  $t$  test; ††,  $p < 0.01$  relative to gp120 alone (untreated), ANOVA with Bonferroni post-test. B, IL-1 $\beta$ -induced synapse loss is mediated by a Src family tyrosine kinase and NMDA receptors. Bar graph summarizes changes in PSD95-GFP puncta (PSDs) after 24-h treatment under control conditions (□) or after treatment with 3 ng/ml IL-1 $\beta$  (■) in the absence (untreated;  $n = 12$ ) or presence of the indicated inhibitors. Cultures were treated with 1  $\mu$ g/ml IL-1-ra ( $n = 9$ ), 10  $\mu$ M MK801 ( $n = 11$ ), 1  $\mu$ M AMD3100 ( $n = 9$ ), or 10  $\mu$ M pyrazolopyrimidine 2 ( $n = 7$ ) as indicated. Data are expressed as mean  $\pm$  S.E.M. \*\*\*,  $p < 0.001$  relative to control Student's  $t$  test; †,  $p < 0.05$  relative to IL-1 $\beta$  alone (untreated), ANOVA with Bonferroni post-test.

gp120 (●). Data are expressed as mean  $\pm$  S.E.M. ( $n \geq 4$  for each data point). \*\*,  $p < 0.01$  relative to PSDs counted before the addition of gp120 (0 h), repeated-measures ANOVA with Bonferroni post test. C, plot shows concentration-dependent changes in the number of PSD95-GFP puncta for cells treated with the indicated concentration of gp120. The mean  $\pm$  S.E.M. of the net change in PSD95-GFP puncta 24 h after treatment with gp120 is plotted for the concentrations indicated ( $n \geq 4$  for each data point). The curve was fit by a logistic equation of the form % PSD change =  $[(A_1 - A_2)/(1 + (X/EC_{50})^p)] + A_2$ , where  $X$  = gp120 concentration,  $A_1 = 31 \pm 8\%$  PSD change without gp120,  $A_2 = -22 \pm 5\%$  PSD change at a maximally effective gp120 concentration, and  $p$  = slope factor.  $EC_{50}$  was calculated using a nonlinear, least-squares curve-fitting program.  $EC_{50}$  and  $p$  were  $153 \pm 50$  pM and  $2 \pm 2$  respectively. D, gp120-induced cell death. Cell death was measured using the PI fluorescence assay detailed under *Materials and Methods*. Cell death was measured after 24 h (squares) and 48 h (circles) treatment with the indicated concentrations of gp120. PI fluorescence was normalized to that measured from cells treated with 1 mM glutamate (100%) with PI fluorescence from untreated wells subtracted (0%). The 24- and 48-h curves were fit to logistic equations resulting in  $EC_{50}$  and  $p$  values of  $68 \pm 77$  pM and  $3 \pm 8$  (24 h), and  $85 \pm 44$  pM and  $0.6 \pm 0.1$  (48 h).



pathway (Kim et al., 2008a; Waataja et al., 2008). Thus, here we determined whether gp120 might induce the loss of PSD95-GFP puncta by activating a ubiquitin ligase. Murine double minute 2 (Zhang et al., 1998) is an E3 ligase present in dendritic spines and known to ubiquitinate PSD95, targeting it for proteasomal degradation (Colledge et al., 2003). Nutlin-3 inhibits ubiquitin ligase activity (Kim et al., 2008a) and when applied at a concentration of 100 nM significantly reduced gp120-induced loss of PSDs (Fig. 4, A and B). p14 ARF binds to and inhibits murine double minute 2 (Colledge et al., 2003). Cultured hippocampal neurons were transfected with expression vectors for ARF (pcDNA3-myc-ARF) (Zhang et al., 1998), PSD95-GFP, and DsRed2 as described previously (Kim et al., 2008a). Hippocampal neurons expressing ARF were protected from gp120-induced synapse loss (Fig. 4B). These data suggest that gp120 induces the loss of synaptic connections through activation of an E3 ligase. Furthermore, gp120 did not significantly reduce the number of puncta in cells expressing PSD95 $\Delta$ PEST-GFP. This construct lacks the PEST sequence at the N terminus of PSD95 that is required for ubiquitination (Colledge et al., 2003). Thus, our results suggest that gp120-induced synapse loss results from NMDA receptor-mediated activation of the ubiquitin-proteasome pathway as described for other excitotoxic stimuli (Kim et al., 2008a,b; Waataja et al., 2008). Neuronal nitric-oxide synthase (nNOS) mediates neuronal death triggered by gp120 (Dawson et al., 1993). However, treatment with *N*<sup>G</sup>-nitro-L-arginine methyl ester hydrochloride (L-NAME), an inhibitor of nNOS, 15 min before and during 24-h exposure to gp120 did not significantly affect PSD loss (Fig. 4B). This result suggests that separate pathways downstream of the NMDA receptor mediate synapse loss and cell death.

We tested this hypothesis using cell survival assays to determine whether gp120-induced neuronal death and synapse loss would show distinct pharmacological profiles (Fig. 4C). Cell death induced by various concentrations of gp120 was quantified by uptake of propidium iodide measured after 48-h exposure. L-NAME (100  $\mu$ M) blocked gp120-induced neurotoxicity, consistent with previous reports (Dawson et al., 1993). In contrast, treatment with nutlin-3 (100 nM) did not significantly affect the gp120 concentration-response curve ( $EC_{50} = 11 \pm 2$  pM) relative to control ( $EC_{50} = 11 \pm 9$  pM). This concentration of nutlin-3 blocked gp120-induced

PSD loss (Fig. 4B). These findings suggest that a path different from that leading to neuronal death mediates the synapse loss induced by gp120.

**Cannabinoid Receptor Agonists Inhibit gp120-Induced Synapse Loss.** Cannabinoids modulate neurotoxic and inflammatory processes (Stella, 2009). Thus, we examined the effects of cannabinoids on HIV protein-induced synapse loss. The cannabinoid receptor full agonist Win55212-2 inhibited synapse loss induced by gp120 (Fig. 5, A and B) but not that evoked by the HIV-1 protein Tat. We examined the effects of cannabinoid receptor antagonists to determine whether the protection of synapses afforded by Win55212-2 was mediated via type 1 or 2 cannabinoid receptors (CB1 or CB2). The selective CB1 antagonist rimonabant did not affect the action of Win55212-2 on gp120-induced synapse loss. In contrast, the CB2 antagonist AM630 (100 nM) blocked the protection from gp120-induced synapse loss afforded by Win55212-2, indicating that the effects of Win55212-2 are mediated by CB2. Because CB2 receptors are expressed by activated microglia, but not hippocampal neurons, our results are consistent with an initial involvement of microglia in the toxic affect of gp120 (Stella, 2010).

**Cannabinoids Inhibit gp120-Induced IL-1 $\beta$  Production in Microglia.** Cannabinoids act on glia and neurons to inhibit the release of proinflammatory molecules (Sheng et al., 2009; Stella, 2009). Thus, we examined the effects of cannabinoids on the production and release of IL-1 $\beta$ . gp120 evoked the expression of IL-1 $\beta$  mRNA by 12 h (Fig. 3B). This increase was blocked by Win55212-2 (Fig. 5C). AM630, but not rimonabant, antagonized the protective effects of Win55212-2 on IL-1 $\beta$  mRNA expression induced by gp120 (Fig. 5C), consistent with CB2 receptors mediating the effects of Win55212-2 on gp120-induced synapse loss.

## Discussion

The synaptic network that forms between hippocampal neurons in culture was significantly degraded after exposure to the HIV envelope protein gp120. The loss of synaptic connections resulted from the indirect mechanism summarized in Fig. 6. gp120 acted on microglia to release the inflammatory cytokine IL-1 $\beta$  with subsequent activation of the NMDA receptor and a ubiquitin ligase. This pathway presents several targets for pharmacological modulation, includ-

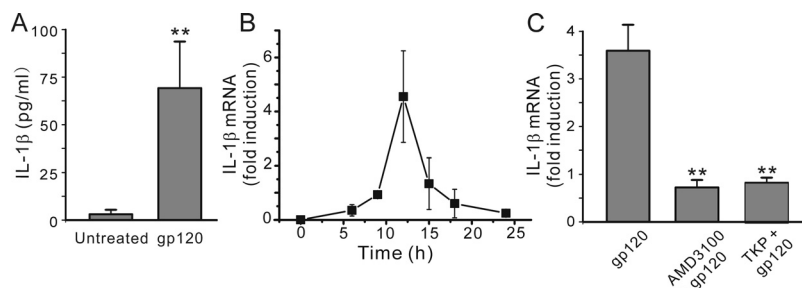


**Fig. 3.** gp120 induced IL-1 $\beta$  production in hippocampal cultures. A, incubation with 600 pM gp120 for 24 h induced the release of IL-1 $\beta$  in rat hippocampal cultures. IL-1 $\beta$  expression was measured by ELISA as described under *Materials and Methods*. gp120-evoked IL-1 $\beta$  levels in hippocampal cultures were near the limit of detection with commercially available ELISAs. Data are expressed as mean  $\pm$  S.E.M. ( $n = 9$ ). \*\*,  $p < 0.01$  relative to control, Student's  $t$  test. B, time course for IL-1 $\beta$  mRNA induction in hippocampal cultures. IL-1 $\beta$  mRNA expression peaked 12 h after treatment with 600 pM gp120 ( $n \geq 3$  for each data point). IL-1 $\beta$  mRNA expression was measured by qRT-PCR as described under *Materials and Methods*. C, induction of IL-1 $\beta$  mRNA was attenuated by inhibition of microglia activation or blocking CXCR4. Bar graph summarizes the effects of inhibitors on changes in the expression of IL-1 $\beta$  mRNA induced by 12-h treatment with 600 pM gp120 (gp120,  $n = 12$ ). TKP (50  $\mu$ M) ( $n = 6$ ) or 1  $\mu$ M AMD3100 ( $n = 8$ ) was applied 15 min before and during treatment with gp120. Data are expressed as mean  $\pm$  S.E.M. \*\*,  $p < 0.01$  relative to gp120 alone (gp120), ANOVA with Bonferroni post test.

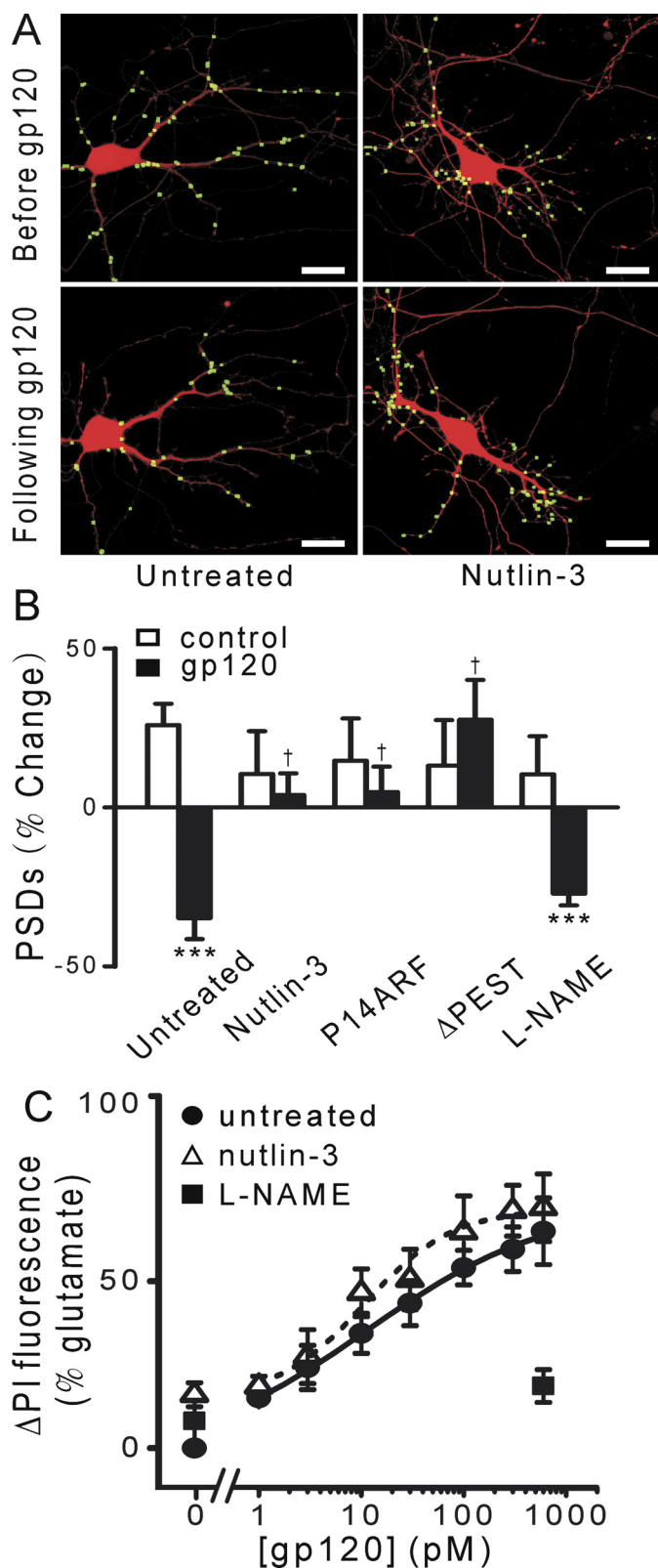


**Fig. 4.** gp120 induced PSD loss via the ubiquitin-proteasome pathway and induced cell death by activating NOS. **A**, processed images display labeled PSDs superimposed on DsRed2 fluorescence acquired before and after 24-h treatment with 600 pM gp120 in control cultures (untreated) and cultures pretreated with 100 nM nutlin-3. Scale bars, 10  $\mu$ m. **B**, bar graph summarizes changes in PSD-GFP puncta (PSDs) after 24-h treatment under control conditions (□) or after treatment with 600 pM gp120 (■) in the absence (untreated,  $n = 24$ ) or presence of inhibitors. Cells were treated with 100 nM nutlin-3 ( $n = 8$ ) or 100  $\mu$ M L-NAME ( $n = 7$ ) 15 min

ing CB2 receptors; CB2 agonists proved to be effective neuroprotective agents.

gp120-induced synapse loss was initiated by binding to CXCR4, which is consistent with the tropism of the IIIB strain of HIV from which the gp120 used in this study was derived. CXCR4 is expressed on microglia, neurons, and astrocytes (Li and Ransohoff, 2008). Activation of CXCR4 produces direct prosurvival effects on neurons (Nicolai et al., 2010) and indirect neurotoxic effects (Bezzi et al., 2001). The balance of prosurvival and neurotoxic effects depends on the specific ligand and the activation state and proximity of surrounding glia. The  $EC_{50}$  for gp120-induced synapse loss was  $153 \pm 50$  nM, in excellent agreement with previous *in vitro* studies (Viviani et al., 2006) and the  $EC_{50}$  of  $85 \pm 44$  pM for gp120-induced cell death agreed with previous cell survival assays (Chun et al., 2009). In studies in which exogenous glutamate was applied to the culture picomolar potencies for gp120 have been reported previously (Dawson et al., 1993). TKP, which inhibits microglial activation (Auriant et al., 1983), prevented gp120-induced synapse loss, suggesting that activation of CXCR4 on microglia was responsible for the gp120-evoked response described here. Activation of CXCR4 on macrophages and microglia results in activation of cell signaling pathways, including the release of  $\beta$ -chemokines (Yi et al., 2004). Our results indicate that IL-1 $\beta$  mediates synapse loss. Microglia activation was required for IL-1 $\beta$  release, although it is possible that other cells in this mixed culture also contributed. Indeed, microglia and astrocytes signal to each other via cytokines (Bezzi et al., 2001; Viviani et al., 2006). Because dendritic changes are early events in most chronic neurodegenerative diseases including HAD (Sá et al., 2004), and many neurodegenerative disorders have an inflammatory component, the mechanisms described here may participate broadly in neurodegenerative processes. The mechanism of synapse loss induced by HIV Tat provides an informative comparison with that of gp120. gp120 evokes synapse loss via an indirect mechanism involving immune cells interacting with neurons, whereas Tat seems to act directly (Kim et al., 2008a). Yet both proteins share a common path of killing neurons via the NMDA receptor.

Phosphorylation of the NMDA receptor complex by Src family kinases potentiates channel gating (Salter et al.,

before and during treatment with gp120 as indicated. Cells expressing p14 ARF (ARF;  $n = 12$ ) or PSD95 $\Delta$ PEST-GFP ( $\Delta$ PEST; in lieu of PSD95-GFP;  $n = 7$ ) are indicated. Data are expressed as mean  $\pm$  S.E.M. \*\*\*,  $p < 0.001$  relative to control, Student's  $t$  test; †,  $p < 0.05$  relative to gp120 alone (untreated), ANOVA with Bonferroni post test. **C**, gp120-induced cell death. Cell death was measured using the PI fluorescence assay detailed under *Materials and Methods* after 48-h treatment with the indicated concentrations of gp120 in the absence (untreated, circles,  $n \geq 11$ ) or presence of 100 nM nutlin-3 ( $\Delta$ ,  $n \geq 11$ ) or 100  $\mu$ M L-NAME ( $\blacksquare$ ,  $n \geq 6$ ). PI fluorescence from untreated wells was subtracted from each curve (0%) and normalized to that measured from cells treated for 48 h with 1 mM glutamate (100%). Concentration-response curves were generated by fitting a logistic equation to the data using a nonlinear, least-squares curve fitting program (Origin 6.0; OriginLab Corporation, Northampton, MA) and  $EC_{50}$  values calculated. A logistic equation of the form  $\Delta PI \text{ Fluorescence} = [(A_1 - A_2)/(1 + (X/EC_{50})^p)] + A_2$  where  $X$  is the gp120 concentration,  $A_1$  is the percentage of change in PI fluorescence without gp120,  $A_2$  is the percentage of change in PI fluorescence at maximal gp120 concentration, and  $p$  is the slope factor. Values for  $A_1$ ,  $A_2$ ,  $EC_{50}$ , and  $p$  for untreated and nutlin-3-treated curves were, respectively,  $-2 \pm 5\%$ ,  $62 \pm 12\%$ ,  $11 \pm 9$  pM, and  $0.5 \pm 0.2$  (untreated) and  $13 \pm 1\%$ ,  $60 \pm 2\%$ ,  $11 \pm 2$  pM, and  $1 \pm 0.2$  (nutlin-3). All data are presented as mean  $\pm$  S.E.M. ( $n \geq 6$ ). A set of triplicate wells from a single plating of cells was defined as a single experiment ( $n = 1$ ).

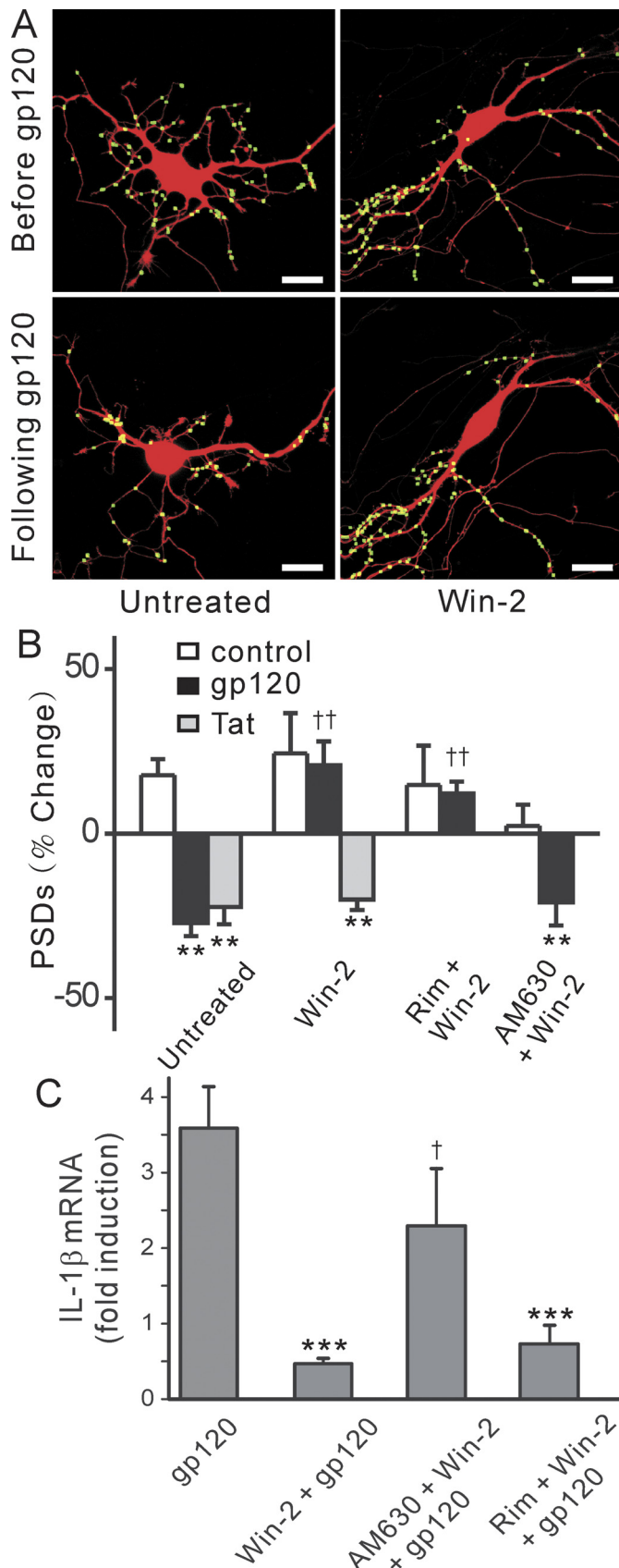


**Fig. 5.** Cannabinoid receptor agonist, Win55,212-2, prevented PSD loss induced by gp120, but not that induced by Tat. A, confocal images show PSD95-GFP puncta before and 24-h after exposure to 600 pM gp120 in the absence (untreated) or presence of Win55,212-2 (Win-2). Scale bars,

2009) and provides a potential link coupling the IL-1 $\beta$  receptor, which is expressed in neurons and activates Src (Viviani et al., 2003), to Ca<sup>2+</sup>-dependent activation of the ubiquitin proteasome pathway. Exposure to NMDA (Waataja et al., 2008), certain epileptiform patterns of activity (Kim et al., 2008b), HIV Tat protein (Kim et al., 2008a), and as shown here, gp120, induced synapse loss via NMDA receptor activation and the ubiquitin-proteasome pathway. This mechanism also mediates certain forms of long-term synaptic depression (Colledge et al., 2003). The increased survival provided by inhibition of nNOS and lack of protection provided by nutlin-3, a drug that prevented synapse loss, suggests that synapse loss is not part of the agonist event but is instead a protective mechanism. The synapse loss described here could represent a coping mechanism that protects the cell from excessive excitatory stimulation analogous to homeostatic scaling.

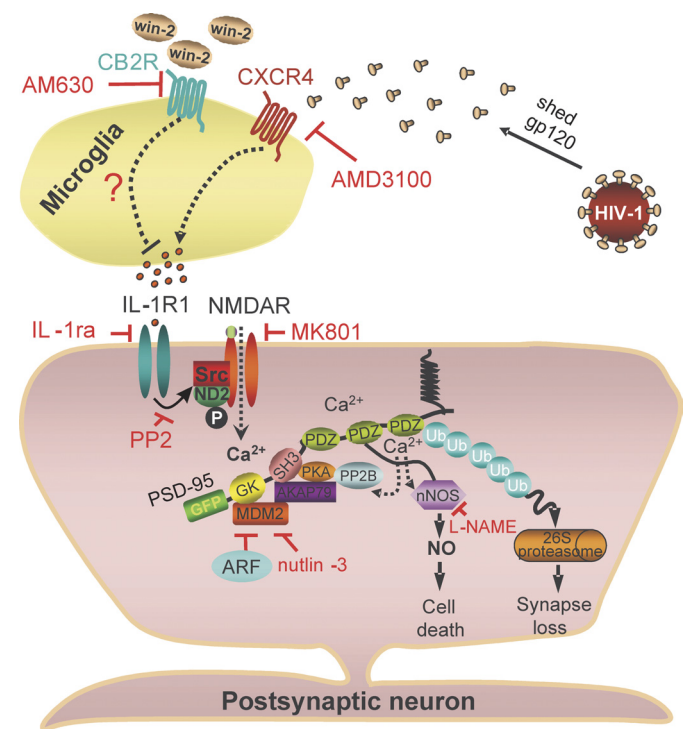


**Fig. 6.** Hypothetical mechanism for gp120-induced synapse loss.

10  $\mu$ m. B, bar graph summarizes changes in PSD95-GFP puncta (PSDs) after 24-h treatment under control conditions (control, □), after treatment with 600 pM gp120 (■), or after treatment with 50 ng/ml Tat (▤). Experiments were performed in the absence ( $n = 18$  for gp120;  $n = 6$  for Tat) or presence of Win-2 ( $n = 15$  for gp120;  $n = 7$  for Tat). The cannabinoid receptor antagonists rimonabant (100 nM;  $n = 15$ ) or AM630 (100 nM;  $n = 16$ ) were applied 5 min before and during exposure to Win-2 and gp120. Data are mean  $\pm$  S.E.M. \*\*,  $p < 0.01$  relative to control; ††,  $p < 0.01$  relative to gp120, ANOVA with Bonferroni post test. C, gp120-evoked IL-1 $\beta$  expression is inhibited by cannabinoids. qRT-PCR was performed as described under Materials and Methods. Bar graph summarizes the effects of cannabinoid receptor ligands on gp120-induced IL-1 $\beta$  mRNA expression. Cultures were treated with 600 pM gp120 in the absence (gp120,  $n = 12$ ) or presence of 100 nM Win-2. Cultures were treated with Win-2 alone (Win-2 + gp120,  $n = 7$ ) or pretreated with 100 nM rimonabant (rim + Win-2 + gp120,  $n = 7$ ) or 100 nM AM630 (AM630 + Win-2 + gp120,  $n = 8$ ) 15 min before and during exposure to gp120 in the presence of gp120. Data are expressed as mean  $\pm$  S.E.M. \*\*\*,  $p < 0.001$  relative to gp120 alone (gp120), Student's  $t$  test; †,  $p < 0.05$  relative to gp120 pretreatment in the presence of gp120 (Win + gp120), ANOVA with Bonferroni post test.



The indirect mechanism of gp120-induced synapse loss highlights the complex multicellular signaling that contributes to neuroinflammatory diseases in general and HAND in particular. Based on the protection from gp120 afforded by TKP, we conclude that the source of IL-1 $\beta$  in our hippocampal cultures is microglia. However, other studies have found that astrocytes release IL-1 $\beta$  in response to gp120 (Viviani et al., 2006). There is also evidence that microglia and astrocytes interact to amplify cytokine-mediated neurotoxicity (Bezzi et al., 2001). The cell culture model described here is well suited to controlling the environment surrounding the neural network to identify the source of these toxic factors. There is evidence implicating viral proteins, proinflammatory cytokines, platelet-activating factor, and excitotoxins in HIV-1 related neuronal death (Kaul et al., 2005), but the role of these factors on the early events that trigger synapse loss are not known and may not track with the cell death mechanisms activated by these agents. The IL-1 $\beta$ -induced synapse loss described here would not only account for the neurotoxicity of shed gp120 but might also account for the effects of HIV-1-infected microglia and macrophages, which exhibit increased IL-1 $\beta$  release (Yadav and Collman, 2009).

The cannabinoid receptor agonist Win55212-2 protected hippocampal cultures from gp120-induced synapse loss. Cannabinoids are of particular relevance to HAND because of their clinical (Plasse et al., 1991) and illicit use (James, 1999) in patients with AIDS. Cannabinoid drugs exhibit neuroprotective properties in excitotoxicity, seizure, and stroke models (Shen and Thayer, 1998; Kim et al., 2008b), and the endocannabinoid system is believed to provide on-demand neuroprotection (Marsicano et al., 2003). Win55212-2 protected hippocampal neurons from gp120-induced synapse loss via a CB2-dependent mechanism. A CB2 agonist reduced immune activation and neuroinflammation in a mouse model of HIV encephalitis (Gorantla et al., 2010), and CB2-mediated anti-inflammatory effects have been described for microglia (Stella, 2009) and astrocytes (Sheng et al., 2009). The release of inflammatory cytokines from HIV-1-infected macrophages and microglia is inhibited by cannabinoids via CB2, CB1, and nonreceptor mechanisms (Stella, 2010). The lack of a CB1 contribution is puzzling in that IL-1 $\beta$  sensitizes the NMDA receptor to glutamate, and thus, synaptic release of glutamate would be expected to contribute to the synapse loss in this model. IL-1 $\beta$  also elevates prostaglandins that can increase presynaptic glutamate release (Marty et al., 2008). The anti-inflammatory effect of cannabinoids shows promise for treating the inflammatory component of neurodegenerative diseases because CB2-selective agonists lack the psychoactive effects of CB1 ligands. Activation of CB2 receptors inhibits CXCR4-mediated chemotaxis in T cells (Ghosh et al., 2006). Both CB2 and CXCR4 are G $_{i/o}$ -coupled receptors. Potential mechanisms by which activation of CB2 receptors might inhibit the signaling of CXCR4 are suggested by the interactions of opiates with CXCR4 and include CXCR4 internalization, the formation of inactive heterodimers, and expression of proteins that inhibit chemokine receptor function (Finley et al., 2008; Pello et al., 2008; Sengupta et al., 2009).

Cognitive decline correlates with dendritic changes in patients with HAD (Sá et al., 2004). Our study suggests that gp120-induced loss of synaptic sites could contribute to early symptoms in patients with HAND. We propose that synapse

loss is a protective mechanism rather than an early step in the progression to cell death. Indeed, synapse loss induced by NMDA receptor activation in our model is reversible (Kim et al., 2008a,b; Waataja et al., 2008). Thus, we suggest that CB2 receptor agonists might reverse the cognitive decline in patients with HAND.

#### Acknowledgments

We thank Dr. Donald B. Arnold and Dr. Yanping Zhang for providing expression plasmids for PSD95-GFP and p14ARF, respectively.

#### Authorship Contributions

*Participated in research design:* Kim, Shin, and Thayer.

*Conducted experiments:* Kim and Shin.

*Performed data analysis:* Kim, Shin, and Thayer.

*Wrote or contributed to the writing of the manuscript:* Kim, Shin, and Thayer.

#### References

- Aurault C, Joseph M, Tartar A, and Capron A (1983) Characterization and synthesis of a macrophage inhibitory peptide from the second constant domain of human immunoglobulin G. *FEBS Lett* **153**:11–15.
- Bezzi P, Domercq M, Brambilla L, Galli R, Schols D, De Clercq E, Vescovi A, Bagetta G, Kollias G, Meldolesi J, et al. (2001) CXCR4-activated astrocyte glutamate release via TNF $\alpha$ : amplification by microglia triggers neurotoxicity. *Nature Neurosci* **4**:702–710.
- Chun H, Hao W, Honghai Z, Ning L, Yasong W, and Chen D (2009) CCL3L1 prevents gp120-induced neuron death via the CREB cell signaling pathway. *Brain Res* **1257**:75–88.
- Colledge M, Snyder EM, Crozier RA, Soderling JA, Jin Y, Langeberg LK, Lu H, Bear MF, and Scott JD (2003) Ubiquitination regulates PSD-95 degradation and AMPA receptor surface expression. *Neuron* **40**:595–607.
- Dawson VL, Dawson TM, Uhl GR, and Snyder SH (1993) Human immunodeficiency virus type 1 coat protein neurotoxicity mediated by nitric oxide in primary cortical cultures. *Proc Natl Acad Sci USA* **90**:3256–3259.
- Donzella GA, Schols D, Lin SW, Esté JA, Nagashima KA, Maddon PJ, Allaway GP, Sakmar TP, Henson G, De Clercq E, et al. (1998) AMD3100, a small molecule inhibitor of HIV-1 entry via the CXCR4 co-receptor. *Nat Med* **4**:72–77.
- Finley MJ, Chen X, Bardi G, Davey P, Geller EB, Zhang L, Adler MW, and Rogers TJ (2008) Bi-directional heterologous desensitization between the major HIV-1 co-receptor CXCR4 and the kappa-opioid receptor. *J Neuroimmunol* **197**:114–123.
- Ghosh S, Preet A, Groopman JE, and Ganju RK (2006) Cannabinoid receptor CB2 modulates the CXCL12/CXCR4-mediated chemotaxis of T lymphocytes. *Mol Immunol* **43**:2169–2179.
- Gorantla S, Makarov E, Roy D, Finke-Dwyer J, Murrin LC, Gendelman HE, and Poluektova L (2010) Immunoregulation of a CB2 receptor agonist in a murine model of neuroAIDS. *J Neuroimmune Pharmacol* **5**:456–468.
- Heaton RK, Franklin DR, Ellis RJ, McCutchan JA, Letendre SL, Leblanc S, Corkran SH, Duarte NA, Clifford DB, Woods SP, et al. (2011) HIV-associated neurocognitive disorders before and during the era of combination antiretroviral therapy: differences in rates, nature, and predictors. *J Neurovirol* **17**:3–16.
- Hesselgesser J, Taub D, Baskar P, Greenberg M, Hoxie J, Kolson DL, and Horuk R (1998) Neuronal apoptosis induced by HIV-1 gp120 and the chemokine SDF-1  $\alpha$  is mediated by the chemokine receptor CXCR4. *Curr Biol* **8**:595–598.
- Ilyin SE and Plata-Salamán CR (1997) HIV-1 envelope glycoprotein 120 regulates brain IL-1 $\beta$  system and TNF- $\alpha$  mRNAs in vivo. *Brain Res Bull* **44**:67–73.
- James JS (1999) Medical marijuana: AIDS-related information in the new Federal report. *AIDS Treat News* **319**:6–8.
- Kaul M and Lipton SA (1999) Chemokines and activated macrophages in HIV gp120-induced neuronal apoptosis. *Proc Natl Acad Sci USA* **96**:8212–8216.
- Kaul M, Zheng J, Okamoto S, Gendelman HE, and Lipton SA (2005) HIV-1 infection and AIDS: consequences for the central nervous system. *Cell Death Differ* **12** (Suppl 1):878–892.
- Kim HJ, Martemyanov KA, and Thayer SA (2008a) Human immunodeficiency virus protein Tat induces synapse loss via a reversible process that is distinct from cell death. *J Neurosci* **28**:12604–12613.
- Kim HJ, Waataja JJ, and Thayer SA (2008b) Cannabinoids inhibit network-driven synapse loss between hippocampal neurons in culture. *J Pharmacol Exp Ther* **325**:850–858.
- Li M and Ransohoff RM (2008) Multiple roles of chemokine CXCL12 in the central nervous system: a migration from immunology to neurobiology. *Prog Neurobiol* **84**:116–131.
- Marsicano G, Goodenough S, Monory K, Hermann H, Eder M, Cannich A, Azad SC, Cascio MG, Gutiérrez SO, van der Stelt M, et al. (2003) CB1 cannabinoid receptors and on-demand defense against excitotoxicity. *Science* **302**:84–88.
- Marty V, El Hachmane M, and Amédée T (2008) Dual modulation of synaptic transmission in the nucleus tractus solitarius by prostaglandin E2 synthesized downstream of IL-1 $\beta$ . *Eur J Neurosci* **27**:3132–3150.
- Merrill JE, Koyanagi Y, Zack J, Thomas L, Martin F, and Chen IS (1992) Induction of interleukin-1 and tumor necrosis factor alpha in brain cultures by human immunodeficiency virus type 1. *J Virol* **66**:2217–2225.
- Nam KN, Koketsu M, and Lee EH (2008) 5-Chloroacetyl-2-amino-1,3-selenazoles

- attenuate microglial inflammatory responses through NF-kappaB inhibition. *Eur J Pharmacol* **589**:53–57.
- Nicolai J, Burbassi S, Rubin J, and Meucci O (2010) CXCL12 inhibits expression of the NMDA receptor's NR2B subunit through a histone deacetylase-dependent pathway contributing to neuronal survival. *Cell Death Disease* **1**:e33.
- Pattarini R, Pittaluga A, and Raiteri M (1998) The human immunodeficiency virus-1 envelope protein gp120 binds through its V3 sequence to the glycine site of *N*-methyl-D-aspartate receptors mediating noradrenaline release in the hippocampus. *Neuroscience* **87**:147–157.
- Pello OM, Martínez-Muñoz L, Parrillas V, Serrano A, Rodríguez-Frade JM, Toro MJ, Lucas P, Monterrubio M, Martínez-A C, and Mellado M (2008) Ligand stabilization of CXCR4/delta-opioid receptor heterodimers reveals a mechanism for immune response regulation. *Eur J Immunol* **38**:537–549.
- Plasse TF, Gorter RW, Krasnow SH, Lane M, Shepard KV, and Wadleigh RG (1991) Recent clinical experience with dronabinol. *Pharmacol Biochem Behav* **40**:695–700.
- Sá MJ, Madeira MD, Ruela C, Volk B, Mota-Miranda A, and Paula-Barbosa MM (2004) Dendritic changes in the hippocampal formation of AIDS patients: a quantitative Golgi study. *Acta Neuropathol (Berl)* **107**:97–110.
- Salter MW, Dong Y, Kalia LV, Liu XJ, and Pitcher G (2009) Regulation of NMDA Receptors by Kinases and Phosphatases, in *Biology of the NMDA Receptor* (Van Dongen AM ed), CRC Press, Boca Raton, FL.
- Schneider J, Kaaden O, Copeland TD, Oroszlan S, and Hunsmann G (1986) Shedding and interspecies type sero-reactivity of the envelope glycopolyptide gp120 of the human immunodeficiency virus. *Journal of General Virology* **67**:2533–2538.
- Sengupta R, Burbassi S, Shimizu S, Cappello S, Vallee RB, Rubin JB, and Meucci O (2009) Morphine increases brain levels of ferritin heavy chain leading to inhibition of CXCR4-mediated survival signaling in neurons. *J Neurosci* **29**:2534–2544.
- Shen M and Thayer SA (1998) Cannabinoid receptor agonists protect cultured rat hippocampal neurons from excitotoxicity. *Mol Pharmacol* **54**:459–462.
- Sheng WS, Hu S, Ni HT, Rock RB, and Peterson PK (2009) WIN55,212–2 inhibits production of CX3CL1 by human astrocytes: involvement of p38 MAP kinase. *J Neuroimmune Pharmacol* **4**:244–248.
- Stella N (2009) Endocannabinoid signaling in microglial cells. *Neuropharmacology* **56** (Suppl 1):244–253.
- Stella N (2010) Cannabinoid and cannabinoid-like receptors in microglia, astrocytes, and astrocytomas. *Glia* **58**:1017–1030.
- Toggas SM, Masliah E, Rockenstein EM, Rall GF, Abraham CR, and Mucke L (1994) Central nervous system damage produced by expression of the HIV-1 coat protein gp120 in transgenic mice. *Nature* **367**:188–193.
- Viviani B, Bartsaghi S, Gardoni F, Vezzani A, Behrens MM, Bartfai T, Binaglia M, Corsini E, Di Luca M, Galli CL, et al. (2003) Interleukin-1beta enhances NMDA receptor-mediated intracellular calcium increase through activation of the Src family of kinases. *J Neurosci* **23**:8692–8700.
- Viviani B, Gardoni F, Bartsaghi S, Corsini E, Facchi A, Galli CL, Di Luca M, and Marinovich M (2006) Interleukin-1 beta released by gp120 drives neural death through tyrosine phosphorylation and trafficking of NMDA receptors. *J Biol Chem* **281**:30212–30222.
- Waataja JJ, Kim HJ, Roloff AM, and Thayer SA (2008) Excitotoxic loss of post-synaptic sites is distinct temporally and mechanistically from neuronal death. *J Neurochem* **104**:364–375.
- Yadav A and Collman RG (2009) CNS inflammation and macrophage/microglial biology associated with HIV-1 infection. *J Neuroimmune Pharmacol* **4**:430–447.
- Yi Y, Lee C, Liu QH, Freedman BD, and Collman RG (2004) Chemokine receptor utilization and macrophage signaling by human immunodeficiency virus type 1 gp120: Implications for neuropathogenesis. *J Neurovirol* **10** (Suppl 1):91–96.
- Zhang Y, Xiong Y, and Yarbrough WG (1998) ARF promotes MDM2 degradation and stabilizes p53: ARF-INK4a locus deletion impairs both the Rb and p53 tumor suppression pathways. *Cell* **92**:725–734.

---

**Address correspondence to:** Dr. Stanley A. Thayer, Department of Pharmacology, University of Minnesota, 6-120 Jackson Hall, 321 Church Street SE, Minneapolis, MN 55455. E-mail: sathayer@umn.edu

---